A Density Functional Theory Study of the Benzene−Water Complex

Shen Li,*,† Valentino R. Cooper,† T. Thonhauser,†,‡ Aaron Puzder,†,§ and David C. Langreth†

Department of Physics and Astronomy, Rutgers University, Piscataway, New Jersey 08854; Department of Materials Science and Engineering, MIT, Cambridge, Massachusetts 02139; and Lawrence Livermore National Laboratory, Livermore, California 94550

Received: February 26, 2008; Revised Manuscript Received: June 30, 2008

The intermolecular interaction of the benzene−water complex is calculated using real-space pseudopotential density functional theory utilizing a van der Waals density functional. Our results for the intermolecular potential energy surface clearly show a stable configuration with the water molecule standing above or below the benzene with one or both of the H atoms pointing toward the benzene plane, as predicted by previous studies. However, when the water molecule is pulled outside the perimeter of the ring, the configuration of the complex becomes unstable, with the water molecule attaching in a saddle point configuration to the rim of the benzene with its O atom adjacent to a benzene H. We find that this structural change is connected to a change in interaction from H (water)/π cloud (benzene) to O (water)/H (benzene). We compare our results for the ground-state structure with results from experiments and quantum-chemical calculations.

1. Introduction

Many properties of biological systems such as the structure of proteins, the structure and function of biopolymers, and molecular recognition processes are influenced by the interaction between aromatic molecules and water. Thus, a molecular-level study of the characteristics of these interactions can lead to a better understanding of many fundamental phenomena.[1] Water can interact with aromatic molecules in several ways. Both H atoms and the O nonpaired electrons in H_2O can participate in forming bonds between molecules. Most aromatic compounds are immiscible in water, which indicates that the magnitudes of the interactions between water and aromatic molecules are very weak.

Benzene has the simplest structure of the aromatic family. Many theoretical and experimental investigations have been done for the benzene−water complex. Suzuki et al. first indicated that benzene can form weak hydrogen bonds with water.[2] The hydrogen bond is the dipole−dipole interaction between a proton donor and a proton acceptor. The typical hydrogen bond is stronger than the van der Waals bond but weaker than covalent or ionic bonds. It had been speculated for years that aromatic hydrocarbons can play the role of proton acceptors.[3] Rotationally resolved spectra of the benzene−water complex showed that the water molecule is positioned above the benzene plane with both H atoms pointing toward the π cloud.[2,4] Although the H positions were not directly located in those experiments, they provided strong evidence for an interaction between the proton donors (H atoms in water) and the proton acceptors (the benzene π cloud).

From a theoretical point of view, second-order Møller−Plesset perturbation theory (MP2) and coupled cluster (CCSD(T)) calculations have been performed for several specific benzene−water configurations.[2,5−12] The two most studied configurations are that of water positioned above the center of the benzene ring with both H atoms equally pointing toward the benzene and that of water positioned above the center of the benzene ring with a single H atom pointing toward the benzene and the other pointing away from it. Most of these calculations indicated that the latter configuration is more stable, though the energy difference between the two configurations is very small. In addition, other computational methods such as molecular dynamics simulation have been used to investigate the properties of the benzene−water complex.[13−16] However, because of the number of degrees of freedom and the computational cost of such calculations, no complete picture of the intermolecular potential energy surface has been reported so far.

To explore the whole potential energy surface, an accurate but efficient theoretical method is needed. For many years, density functional theory (DFT) has been widely accepted as an useful tool to understand and predict the electronic properties of materials. Compared to quantum-chemical methods such as MP2 or CCSD(T), standard DFT methods are often a better choice for large-sized systems because of the computational cost. It is efficient, and for both dense matter and isolated molecules, it typically has sufficient accuracy. Nevertheless, for van der Waals (vdW) complexes and sparse matter, where the dispersion energy is important, standard density functionals are typically inadequate. This is also certainly true for benzene−water, where Zimmerli et al.[17] have shown that standard functionals such as BLYP, B3LYP, PBE, etc., give inadequate binding. A Hartree−Fock calculation[10] also gives inadequate binding.

To remedy the situation, a van der Waals density functional (vdW-DF) has been developed which can approximately treat long-range dispersion interaction.[18,19] This is a regular density functional using a generalized-gradient type exchange functional, combined with a fully nonlocal correlation functional of the form

$$E_c^{nl} = \frac{1}{2}\int d^3\vec{r}\, d^3\vec{r}\,'\, \rho(\vec{r})\, \Phi(\vec{r},\vec{r}\,')\, \rho(\vec{r}\,') \qquad (1)$$

where $\rho(\vec{r})$ is the electronic charge density and where the kernel $\Phi(\vec{r},\vec{r}\,')$ depends on the charge density and its gradient at the points $\vec{r}$ and $\vec{r}\,'$. It contains no empirical input. Of methods that include London dispersion, it occupies a middle ground between

* To whom correspondence should be addressed.
† Rutgers University.
‡ MIT.
§ Lawrence Livermore National Laboratory.

10.1021/jp801693p CCC: $40.75
Published on Web 08/27/2008

fully ab initio wave function methods and methods that add a dispersion component to ordinary DFT via empirical or semiempirical force fields acting pairwise between the nuclei. The latter methods have their origin long ago,[20,21] and recently many variations have been developed and applied; see Grimme et al.[22] for a review. Such methods have previously been applied[17] to the benzene−water dimer. These authors characterize their work as "far from generally applicable" and "having to be tailored to the problem in question". On the other hand, vdW-DF has obtained useful results for a wide range of problems (see next paragraph) with no change whatever in the functional. The vdW-DF has the same scaling with system size as the latter methods and like them is capable of application to much larger systems than are feasible with the ab initio wave function methods.

The vdW-DF has been applied to a number of vdW systems. These range from relatively simple complexes[18,19,23−25] to large system applications including the physisorption of benzene and naphthalene on graphite,[26] the structure of a polymer crystal,[27] the prediction of the twist of DNA,[28,29] and the adsorption of benzene on a semiconductor surface.[30] Variants of the method have been applied to adsorption of organics on metallic surfaces[31,32] and to potassium intercalation in graphite.[33] For a system of the size considered in the present paper, there are of course many methods which could be used, and these have been reviewed by some of us in recent publications.[19,23] Of these, vdW-DF is unique in being a fully nonempirical density functional for the nonlocal correlation energy which scales with system size as ordinary DFT. The present calculations open the way for applications of vdW-DF to the interaction of water with much larger aromatic systems.

In this paper, we report our study of the benzene−water intermolecular potential energy surface using a real-space pseudopotential DFT method employing the vdW-DF. The ground-state structure is determined, and the properties of different interactions are discussed. Where appropriate, we compare our results with experimental and theoretical results. Our purpose is not only to benchmark the vdW-DF functional but also to get insight into the benzene−water complex and explore the possible applications for this functional.

2. Computational Details

VdW-DF can be implemented in two different ways: (i) self-consistently, where the exchange-correlation potential corresponding to the nonlocal vdW-DF is included as part of the Kohn−Sham potential and the charge density used to evaluate the energy is fully self-consistent, and (ii) non-self-consistently, where the nonlocal correlation energy is evaluated as a post-processing perturbation, using a charge density obtained from self-consistent calculations with Perdew−Burke−Ernzerhof (PBE)[34] or revised PBE (revPBE) functionals.[35] As found by Thonhauser et al.,[19] our results indicate the self-consistent and non-self-consistent implementations lead to nearly indistinguishable results because the van der Waals interaction is so weak and diffuse that it does not substantially change the electronic charge distribution.

Here, we implemented vdW-DF within the code PARSEC,[36] which is based on self-consistently solving the Kohn−Sham equations on a uniform, real-space grid. This method has a number of advantages. For example, since no supercell geometry or periodic boundary is involved, one can study van der Waals complexes with dipole moments or net charges more efficiently. Furthermore, as compared with localized basis methods, the choice of basis set is not an issue; one simply decreases the grid spacing until convergence is obtained. Here, we found that an accuracy of 0.02 kcal/mol could be obtained with a grid spacing of 0.3 bohr (b). The convergence is illustrated in Table 1. We used Troullier−Martins pseudopotentials.[37] The molecules were placed at the center of a spherical domain large enough so that all the wave functions vanish smoothly at the boundary. For these calculations, we used a spherical radius of 16 b. Table 1 shows that it is sufficient for our calculations.

TABLE 1: Convergence Test for the Configuration Shown in Figure 2

Spherical Radius = 16 b	
grid spacing (b)	interaction energy (kcal/mol)
0.65	−4.20
0.60	−3.79
0.55	−2.53
0.50	−2.84
0.45	−2.86
0.40	−2.68
0.35	−2.67
0.30	−2.69
0.25	−2.68
0.20	−2.68
Grid Spacing = 0.3 b	
spherical radius (b)	interaction energy (kcal/mol)
13	−2.70
14	−2.69
15	−2.69
16	−2.69
17	−2.69
18	−2.69
19	−2.69
20	−2.69

The computational cost of one electronic self-consistent run for the benzene−water complex on one opteron processor is ∼1.32 h for PBE, 1.42 h for non-SC vdW-DF, and 4.20 h for SC vdW-DF. Since the computational cost of non-SC vdW-DF is comparable to PBE, it can be feasibly applied to any system that PBE can handle. Since the PBE cost scales roughly as the cube of the system size, while the evaluation of E_c^{nl} in eq 1 scales as the square of this size, the fractional increase in cost of vdW-DF (non-SC or SC) becomes smaller and smaller as the system size increases.

We first optimized the ground-state structure for the individual molecules using PBE. The H−O bond lengths and H−O−H angle for the water molecule were found to be 0.973 Å and 106°, respectively, where the corresponding experimental values are 0.958 Å and 104.5°.[38] For the dipole moment of water we find 1.78 D, in comparison to the experimental value of 1.85 D.[38−40] Other PBE calculations gave 1.81 and 1.80 D.[41,42] Our C−C and C−H bond lengths for the benzene molecule were 1.396 and 1.100 Å, respectively. The corresponding experimental results are 1.397 Å for C−C and 1.084 Å for C−H.[38] We also calculated the quadrupole moment of benzene. The traceless quadruple tensor is given by $2\Theta_{ij} = Q_{ij} = \int(3r_ir_j - r^2\delta_{ij})\rho(r)\, d^3r$, where the subscripts label Cartesian components and δ_{ij} is the unit tensor. Here Θ_{ij} is the definition given by Buckingham,[43] while Q_{ij} is used by Jackson.[44] Taking the axial symmetry direction along the $z \equiv r_3$ axis implies via the traceless property that $\Theta \equiv \Theta_{33} = -2\Theta_{22} = -2\Theta_{11}$. From our calculation, the quadrupole moment of benzene is $\Theta = -5.60$ au, which is in the range of previously calculated DFT values.[45] The experimental value is -6.31 ± 0.26 au.[46] An MP2 calculation[47] gives −7.11 au.

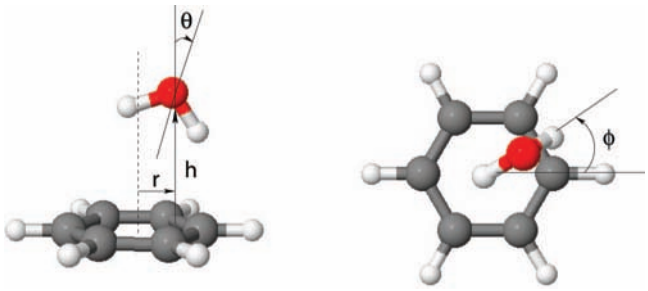

Figure 1. Definition of the degrees of freedom used for the benzene−water complex. We assume that the water plane is perpendicular to the benzene and cuts through the center of the benzene ring. The quantity h is the distance between the O atom and the benzene plane; r is the horizontal displacement between the O atom and the center of benzene; θ is the tilting angle of water between the C_2 axis and the vertical line; ϕ is the rotation angle of the water plane along the C_6 axis of benzene.

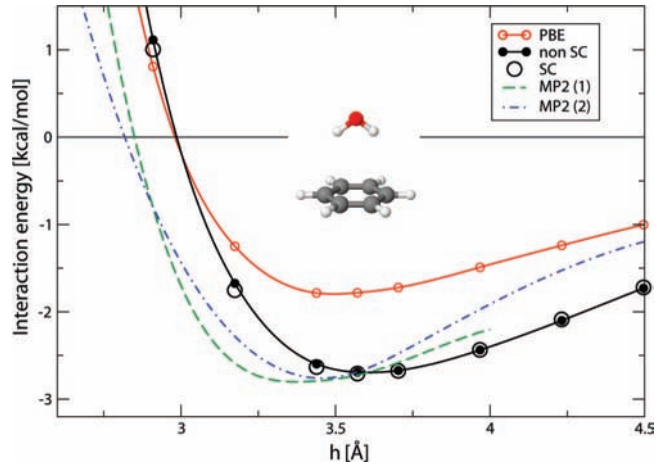

Figure 2. Interaction energy as a function of h. The configuration studied corresponds to $r = 0$ Å, $\theta = 0°$, and $\phi = 0°$.

The combination of slightly underestimated dipole and quadruple moments implies that the asymptotic interaction energy, which for this system is dominated by the dipole−quadrupole interaction, will be around 15% too weak. The extent to which this translates into weakened electrostatic attraction at equilibrium separation is unclear.

3. Results and Discussion

3.1. Degrees of Freedom. Because of the large number of degrees of freedom of the benzene−water complex, we limit ourselves to the following cases. First, we assume that the structure of each molecule will not change when being put together. Second, we assume that the plane of the water molecule is perpendicular to the plane of benzene, as supported by experiment. Third, because of the symmetry of the benzene ring, we considered only cases where the plane of the water molecule cuts through the center of the benzene ring. With the assumptions above, there are four remaining geometric variables as can be seen in Figure 1: (i) height h, which is the distance between the O atom in water and the benzene plane; (ii) the horizontal displacement r between the O atom in water and the center of the benzene; (iii) the tilting angle θ of the water molecule, which is the angle between the C_2 axis of water and the vertical line. When $\theta = 0°$, the H atoms in water point down at equal angles toward the benzene ring. Finally, we have (iv) the rotation angle ϕ of the water plane along the C_6 axis of benzene. When $\phi = 0°$, the water plane cuts through a C atom and the center of benzene. When $\phi = 30°$, the water plane cuts through the center of benzene and the middle of a C−C bond.

3.2. Height Dependence. We first investigate the configurations with various h. Figure 2 shows the interaction energy as a function of h, while we fixed the other parameters to be $r = 0$ Å, $\theta = 0°$, and $\phi = 0°$. We performed calculations with PBE, self-consistent (SC) vdW-DF, and non-self-consistent (nonSC) vdW-DF. The PBE calculation gave h at the energy minimum as 3.44 Å and the corresponding interaction energy as −1.78 kcal/mol. Our SC vdW-DF and nonSC vdW-DF are almost identical around the equilibrium distance, which is consistent with previous studies.[19] Both of them gave h at the energy minimum as 3.57 Å and the corresponding interaction energy as −2.69 kcal/mol. For this configuration, two MP2 calculations are available, which report 3.4 Å, −2.81 kcal/mol and 3.5 Å, −2.75 kcal/mol, respectively.[10,17]

Obviously, compared with MP2, vdW-DF can give better interaction properties than PBE. Though MP2 calculations gave a shorter equilibrium distance and lower interaction energy than vdW-DF, the difference is less than 5% for both. The overestimation of the equilibrium distance has been found to be a systematic error of the method and has been attributed[23] to differences between the slope of the HF energy curve and that of local exchange functionals tried. Our group has embarked on a systematic effort to develop improvements.

We now turn to a brief discussion of the PBE results. PBE results for this and other geometries have previously been obtained.[17] In contrast to the previous observation that standard GGA functionals, when applied to dispersion bonded systems like benzene dimers[18] or MoS_2 sheets,[48] give equilibrium distances too large by an angstrom or more and binding energies too small by an order of magnitude; here, PBE gives a more acceptable equilibrium distance and a significant part of the binding energy. This indicates that for this particular configuration the interaction between benzene and water molecules may not be pure van der Waals force. This is consistent with the previous claim that the interaction between the benzene π cloud and the H atoms in water can be a weak hydrogen bond. Since SC vdW-DF and nonSC vdW-DF gave indistinguishable interaction properties, we henceforth only present results from nonSC vdW-DF calculations.

3.3. Tilting Angle Dependence. Next, we changed θ of the water molecule while fixing $\phi = 0°$ and $r = 0$ Å. We optimized h for each θ. The interaction energy and optimized h are plotted in Figure 3. We also plotted the results of MP2 calculations.[10] From the plot we can see that the interaction energy curve is flat from $\theta = 0°$ to $\theta = 60°$ (or, equivalently, from $\theta = 300°$ to $\theta = 360°$). The change in the energy is less than 0.15 kcal/mol. The configuration becomes unstable from $\theta = 60°$ to $\theta = 300°$, where both H atoms point away from the benzene ring. Our vdW-DF calculations agree fairly well with the MP2 calculations shown in the figure. Our calculations show that the configuration with $\theta = 30°$ and $h = 3.57$ Å gives the minimum interaction energy, which is −2.72 kcal/mol. The MP2 calculations gave a lower minimum interaction energy (∼−2.8 kcal/mol) at the same θ. Note that in the MP2 calculations h is fixed to 3.4 Å. To compare with MP2, we also calculated the central part of the energy curve with h fixed to 3.4 Å to illustrate the energy gained by optimization. The energy difference between MP2 and our calculation is therefore not significantly due to differences in optimization. It is more likely to be due to electrostatics typified by the weakened PBE quadrupole moment, whose effect is magnified when the water is rotated 180°.

Our results indicate that, although the water molecule prefers tilting at a specific angle, the energy difference is so small that

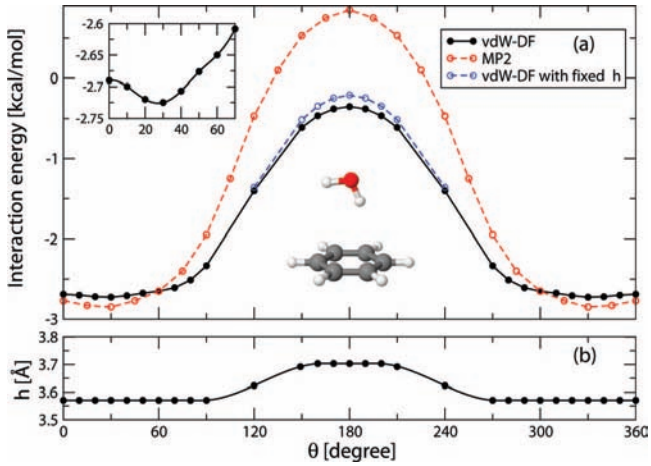

Figure 3. (a) Interaction energy as a function of θ. The configuration studied corresponds to $r = 0$ Å and $\phi = 0°$. For each point we optimized h shown as the solid black curve. The small inset is a magnification of angles up to $\theta = 70°$. The dashed line is taken from an MP2 calculation for $h = 3.4$ Å.[10] The peak around $\theta = 180°$ would presumably have been slightly lower if h used in that calculation had been optimized. The blue curve fragment is a vdW-DF calculation for the central region with fixed height of $h = 3.4$ Å. (b) The optimized h for the vdW-DF calculation.

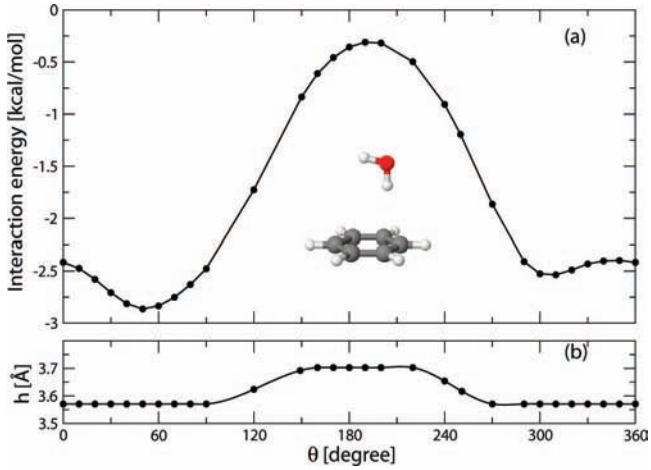

Figure 4. Tilting angle dependence. The configuration studied has $r = 0.8$ Å, $\phi = 0°$. (a) The interaction energy as a function of θ. The minimum at $\theta = 50°$ of -2.86 kcal/mol corresponds to the global minimum in vdW-DF. (b) The correspondingly optimized h.

the water molecule can in fact tilt arbitrarily as long as one or both of the H atoms point toward the π cloud. To test whether or not this is the case for the whole benzene plane, we shifted the water molecule off the center of the benzene ring. The interaction energy and the optimized h are plotted in Figure 4. The configuration corresponds to $r = 0.8$ Å and $\phi = 0°$. Similar to the case in which the water molecule stands above the center of the benzene ring, the variation in the interaction energy curve is small from $\theta = 0°$ to $\theta = 90°$ as well as from $\theta = 290°$ to $\theta = 360°$. The difference in energy is around 0.5 kcal/mol. Again, from $\theta = 90°$ to $\theta = 290°$, when both H atoms point away from the benzene ring, the configuration becomes unstable. The minimum interaction energy is -2.86 kcal/mol at $\theta = 50°$. Further calculations will show that this is the global minimum. As in the previous case, the optimized h is almost constant for all θ.

Our results for the tilting angle dependence of the interaction energy show that when the water molecule stands above the benzene, one or both of the H atoms will point toward the benzene ring. This is consistent with the experimental observations.[2]

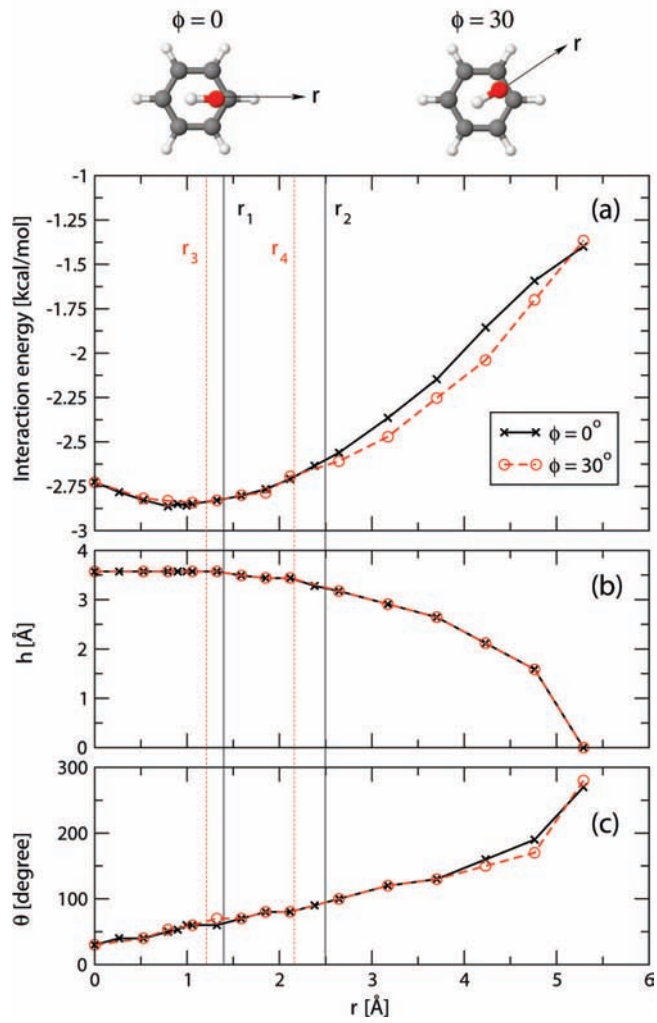

Figure 5. Horizontal displacement dependence. The solid line is for $\phi = 0°$, and the dashed line is for $\phi = 30°$. The quantities r_1 and r_2 are the distance from the center of the benzene ring to the C atom and H atom of the benzene, respectively, while r_3 and r_4 are the respective distances from the center of the benzene ring to the middle of the C−C bond and H−H line of the benzene. (a) The interaction energy. (b) The optimized h. (c) The optimized θ.

3.4. Horizontal Displacement Dependence. More of the intermolecular potential energy surface was explored by shifting the water molecule from the center toward the edge of the benzene ring. Figure 5 displays the interaction energy as a function of r. Both θ and h are optimized. We shifted the water molecule in two directions. First is in the direction of the C atom, which has $\phi = 0°$. The other is in the direction of the middle of the C−C bond, which corresponds to $\phi = 30°$. The position of the C atom, H atom, C−C bond, and the H−H line of benzene are marked in the plot as r_1, r_2, r_3, and r_4, respectively. The corresponding configurations for the $\phi = 0°$ case are shown in Figure 6.

From the plot, we can see that within the benzene ring (left side of the r_2 line marked in Figure 5) the interaction energy curves are very flat. The variation is less than 0.25 kcal/mol. In that region, the optimized h is almost constant for different r. The optimized θ increases with increasing r. The interaction energy, the optimized h, and θ are almost identical for $\phi = 0°$ and $\phi = 30°$. The minimum interaction energy is -2.86 kcal/

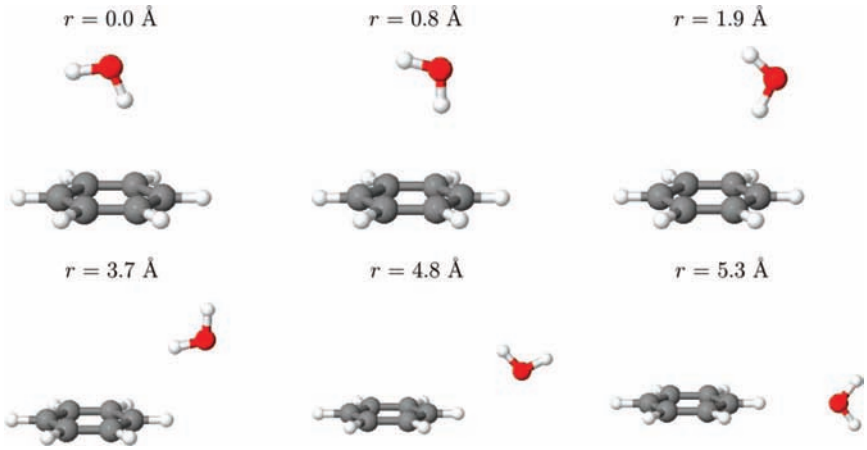

Figure 6. Benzene−water configurations as a function of r. For each value of r, both θ and h are optimized. The configurations plotted have $\phi = 0°$.

mol at $r = 0.8$ Å. The corresponding h and θ are 3.57 Å and 50°, respectively. This is the minimum shown in Figure 4. MP2 at the basis set limit gives about −3.7 kcal/mol when corrected for basis set superposition error.[9,12] An estimate of the CCSD(T) correction is about 0.3 kcal/mol,[10,12] resulting in a best theoretical estimate of about −3.4 kcal/mol. An even more recent calculation[49] gave a value of −3.28 kcal/mol. The vdW-DF value is ∼15% smaller in magnitude than this. To compare with the experimental dissociation energy, one needs to know the zero point energy. This has been estimated to be about 1.0 kcal/mol neglecting anharmonicity,[9] whose importance was suspected. Nevertheless, if one uses this number at face value, and combines it with the two experimental numbers with small error bars[14,50] as done by Zhao et al.,[12] one ends up with the tentative conclusion that there is agreement between the CCSD(T) corrected theoretical value above and experiment.

Our results are consistent with the idea that the π cloud is uniformly distributed around the perimeter of the benzene ring. There is little difference in energy for water to shift toward the direction of C atom or toward the direction of the C−C bond. Also, the interaction profile along the radius is relatively flat. Water can easily move back and forth between the center and the border of the benzene. The water molecule prefers a different θ for each different r; considering the tilting angle dependence of the interaction energy above, water can easily move with any θ that makes one or both of the H atoms point down toward the benzene.

As the water molecule is moved beyond the benzene ring (right side of the r_2 line marked in Figure 5), the complex successively becomes less strongly bound, while the optimized h drops rapidly. At $r = 5.3$ Å, the optimized h becomes zero. The optimized θ increases beyond 180°. From Figure 6, we can see that the water molecule turns upside down with increasing r. At $r = 5.3$ Å, when the optimized h becomes zero, θ is around 270°. The H atoms of water equally point away from the benzene ring. There is an obvious difference in energy for $\phi = 0°$ and $\phi = 30°$. However, at $r = 5.3$ Å, the difference is small again. The corresponding h and θ are almost the same for $\phi = 0°$ and $\phi = 30°$.

Our results for this region show that once the water molecule has been displaced beyond the perimeter of the benzene ring, it no longer interacts with the benzene via its H atoms. Instead, it prefers the interaction of its O atom with the H atoms on the rim of the benzene ring. The configurations in this region are less strongly bound than those involving the interactions between H atoms and π cloud.

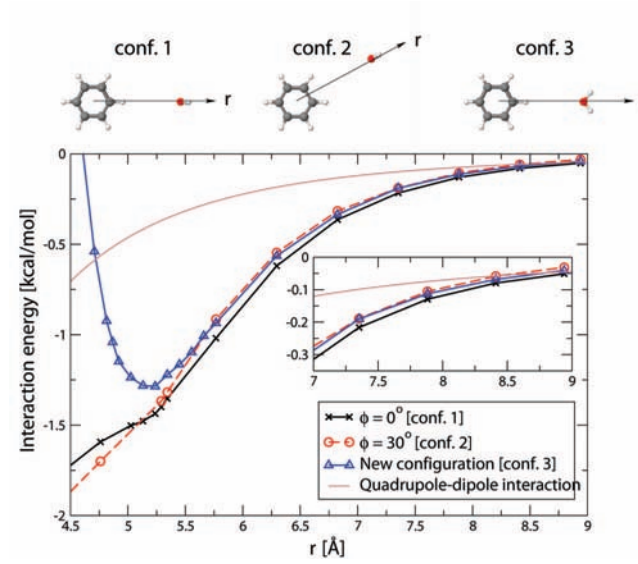

Figure 7. Interaction energy as a function of r. Energy curves for conf. 1 and 2 are the extension of the energy curves in Figure 5. Conf. 3 has h fixed to 0 Å, with the O atom in water pointing toward the H atom in benzene and the H atoms in water pointing away from benzene at equal angles; in this configuration all atoms are coplanar. The brown curve is the calculated quadrupole−dipole interaction. The small inset is a magnification of r from 7 to 9 Å.

To further investigate the properties of O/H interactions, we shifted the water molecule beyond $r = 5.3$ Å. The interaction energy as a function of r is plotted in Figure 7. Conf. 1 and 2 correspond to the configurations with $\phi = 0°$ and 30°, respectively. Their energy curves are the extension of the energy curves in Figure 5. Beyond $r = 5.3$ Å, h and θ are fixed to 0 Å and 270°, respectively. For comparison, we also studied a new configuration (conf. 3). The water and benzene molecules are in the same plane. The O atom in water interact with the H atom in benzene. Both H atoms in water point away from benzene ring at equal angles.

As the water moves to larger distances, the interaction energy becomes dominated by the interaction between the water dipole and the benzene quadrupole. For the geometries of Figure 7, the interaction is attractive and has the magnitude $C|\mu\Theta|/r^4$, where μ is the water dipole moment, Θ is the benzene quadrupole moment as defined earlier, and C is a constant. Using the dipole field gradients in the standard electrostatic expression[44] for their interaction with a quadrupole gives $C = -3/2$ au. The resulting asymptotic expression is plotted in Figure 7

to illustrate that the full interaction energy curves have essentially reached their asymptote at $r \sim 9$ Å.

From Figure 7, we can see that when r is less than 5.3 Å, conf. 1 and 2 have lower energy. Conf. 3 is unstable. Around $r = 5.3$ Å, the energies of the three configurations are nearly equal. The energy curve for conf. 3 has a minimum of −1.29 kcal/mol at 5.3 Å. MP2 calculations gave these values as −0.98 kcal/mol and 4.91 Å.[11] Beyond 5.3 Å, the energy difference between the three configurations is very small.

The energy curves in Figure 7 show clearly that when the water molecule is far beyond the perimeter of the benzene ring, it will interact with the H atoms of the benzene ring through the O atom of the water molecule. The H atoms in water have little influence on these interactions and can rotate freely along the C_2 axis. We also find that the interaction between water and the benzene rim is essentially independent of ϕ in this regime, as expected from symmetry combined with the dominance of the quadrupole−dipole interaction in this regime.

4. Conclusion

Our vdW-DF calculations for the benzene−water complex suggest that either the H atoms or the O atom of water can interact with benzene, depending on the location of the water. When the water molecule is above or below the benzene, it prefers a configuration with at least one H atom interacting with the π cloud. These configurations are quasi-stable. When it is beside the benzene, the water molecule will interact with the rim of the benzene ring via its O atom. These configurations are saddle points.

Our ground-state structure for the benzene−water complex agrees qualitatively with available experiments and quantum chemical wave function calculations, which suggests that vdW-DF is a promising tool for similar weakly interacting systems, especially for much larger systems for which alternative nonempirical methods are unavailable. In particular, it would be interesting to apply vdW-DF to water on polycyclic aromatic hydrocarbons of increasing size. For example, this could bring a completion to the picture whose beginning has been made by Feller and Jordan[51] via MP2. Water on a graphene sheet and/or the surface of graphite could also be simply treated with vdW-DF.

Acknowledgment.

This work was supported in part by NSF Grant DMR-0456937.

References and Notes

(1) (a) Hunter, C. A. *J. Mol. Biol.* **1993**, *230*, 1025. (b) Lehn, J.-M. *Supramolecular Chemistry. Concepts and Perspectives*; VCH: Weinheim, Germany, 1995.

(2) Suzuki, S.; Green, P. G.; Bumgarner, R. E.; Dasgupta, S.; Goddard, W. A., III; Blake, G. A. *Science* **1992**, *257*, 942.

(3) (a) Levitt, M.; Perutz, M. F. *J. Mol. Biol.* **1988**, *201*, 751. (b) Perutz, M. F. In *The Chemical Bond*; Zewail, A., Ed.; Academic Press: New York, 1992; pp 17−30. (c) Burley, S. K.; Petsko, G. A. *FEBS Lett.* **1986**, *203*, 139.

(4) Gutowsky, H. S.; Emilsson, T.; Arunan, E. *J. Chem. Phys.* **1993**, *99*, 4883.

(5) Bródas, J. L.; Street, G. B. *J. Chem. Phys.* **1989**, *90*, 7291.

(6) Cheney, B. V.; Schulz, M. W. *J. Phys. Chem.* **1990**, *94*, 6268.

(7) Fredericks, S. Y.; Jordan, K. D. *J. Phys. Chem.* **1996**, *100*, 7810.

(8) Kim, K. S.; Lee, J. Y.; Choi, H. S.; Kim, J.; Jang, J. H. *Chem. Phys. Lett.* **1997**, *265*, 497.

(9) Feller, D. *J. Phys. Chem. A* **1999**, *103*, 7558.

(10) Tsuzuki, S.; Honda, K.; Uchimaru, T.; Mikami, M.; Tanabe, K. *J. Am. Chem. Soc.* **2000**, *122*, 11450.

(11) Mishra, B. K.; Sathyamurthy, N. *J. Phys. Chem. A* **2007**, *111*, 2139.

(12) Zhao, Y.; Tishchenko, O.; Truhlar, D. G. *J. Phys. Chem. B* **2005**, *109*, 19046.

(13) Tachikawa, H.; Igarashi, M. *J. Phys. Chem. A* **1998**, *102*, 8648.

(14) Courty, A.; Mons, M.; Dimicoli, I.; Piuzzi, F.; Gaigeot, M.; Brenner, V.; Pujo, P.; Millié, P. *J. Phys. Chem. A* **1998**, *102*, 6590.

(15) Dang, L. X.; Feller, D. *J. Phys. Chem. B* **2000**, *104*, 4403.

(16) Allesch, M.; Schwegler, E.; Galli, G. *J. Phys. Chem. B* **2007**, *111*, 1081.

(17) Zimmerli, U.; Parrinello, M.; Koumoutsakos, P. *J. Chem. Phys.* **2004**, *120*, 2693.

(18) Dion, M.; Rydberg, H.; Schröder, E.; Langreth, D. C.; Lundqvist, B. I. *Phys. Rev. Lett.* **2005**, *95*, 109902.

(19) Thonhauser, T.; Cooper, V. R.; Li, S.; Puzder, A.; Hyldgard, P.; Langreth, D. C. *Phys. Rev. B* **2007**, *76*, 125112.

(20) Hepburn, J.; Scoles, G.; and Penco, R. *Chem. Phys. Lett.* **1975**, *36*, 451.

(21) Ahlrichs, R.; Penco, R.; and Scoles, G. *Chem. Phys.* **1977**, *19*, 119.

(22) Grimme, S.; Antony, J.; Schwabe, T.; Mück-Lichtenfeld, C. *Org. Biomol. Chem.* **2007**, *5*, 741.

(23) Puzder, A.; Dion, M.; Langreth, D. C. *J. Chem. Phys.* **2006**, *124*, 164105.

(24) Thonhauser, T.; Puzder, A.; Langreth, D. C. *J. Chem. Phys.* **2006**, *124*, 164106.

(25) Hooper, J.; Cooper, V. R.; Thonhauser, T.; Romero, N. A.; Zerilli, F.; Langreth, D. C. *ChemPhysChem* **2008**, *9*, 891.

(26) Chakarova-Käck, S. D.; Schröder, E.; Lundqvist, B. I.; Langreth, D. C. *Phys. Rev. Lett.* **2006**, *96*, 146107.

(27) Kleis, J.; Lundqvist, B. I.; Langreth, D. C.; Schröder, E. *Phys. Rev. B* **2007**, *76*, 100201(R)

(28) Cooper, V. R.; Thonhauser, T.; Puzder, A.; Schröder, E.; Lundqvist, B. I.; Langreth, D. C. *J. Am. Chem. Soc.* **2008**, *130*, 1304.

(29) Cooper, V. R.; Thonhauser, T.; Langreth, D. C. *J. Chem. Phys.* **2008**, *128*, 204102.

(30) (a) Johnston, K.; Kleis, J.; Lundqvist, B. I.; Nieminen, R. M. *Phys. Rev. B* **2008**, *77*, 121404. (b) Erratum: *Phys. Rev. B* **2008**, *77*, 209904.

(31) Sony, P.; Puschnig, P.; Nabok, D.; Ambrosch-Draxl, C. *Phys. Rev. Lett.* **2007**, *99*, 176401.

(32) Yanagisawa, S.; Lee, K.; Morikawa, Y. *J. Chem. Phys.* **2008**, *128*, 244704.

(33) Ziambaras, E.; Kleis, J.; Schröder, E.; Hyldgaard, P. *Phys. Rev. B* **2007**, *76*, 155425.

(34) Perdew, J. P.; Burke, K.; Ernzerhof, M. *Phys. Rev. Lett.* **1996**, *77*, 3865.

(35) Zhang, Y.; Yang, W. *Phys. Rev. Lett.* **1998**, *80*, 890.

(36) Chelikowsky, J. R.; Troullier, N.; Saad, Y. *Phys. Rev. Lett.* **1994**, *72*, 1240; see http://www.ices.utexas.edu/parsec/

(37) Troullier, N.; Martins, J. L. *Phys. Rev. B* **1991**, *43*, 1993.

(38) *NIST Chemistry Webbook, NIST Standard Reference Database*; Linstrom, P. J., Mallard, W. G., Eds.; National Institute of Standards and Technology: Gaithesburg, MD, 2001; No. 69 (http://webbook.nist.gov).

(39) Dyke, T. R.; Muenter, A. J. *J. Chem. Phys.* **1973**, *59*, 3125.

(40) Shostak, S. L.; Ebenstein, W. R.; Muenter, J. S. *J. Chem. Phys.* **1991**, *94*, 5875.

(41) Xu, X.; Goddard, W. A., III *J. Phys. Chem. A* **2004**, *108*, 2305.

(42) Davidson, E. R.; Eichinger, B. E.; Robinson, B. H. *Opt. Mater.* **2006**, *29*, 360.

(43) Buckingham, A. D. *J. Phys. Chem.* **1959**, *30*, 1580.

(44) Jackson, J. D. *Classical Electrodynamics*, 3rd ed.; Wiley & Sons: New York, 1998.

(45) Meijer, E. J.; Sprik, M. *J. Chem. Phys.* **1996**, *105*, 8684.

(46) Dennis, G. R.; Ritchie, G. L. D. *J. Phys. Chem.* **1991**, *95*, 656.

(47) Hobza, P.; Seizie, H. L.; Schlag, E. W. *J. Am. Chem. Soc.* **1994**, *116*, 3500.

(48) Rydberg, H.; Dion, M.; Jacobson, N.; Schröder, E.; Hyldgaard, P.; Simak, S. I.; Langreth, D. C.; Lundqvist, B. I. *Phys. Rev. Lett.* **2003**, *91*, 126402.

(49) Jurecka, P.; Sponer, J.; Hobza, P. *Phys. Chem. Chem. Phys.* **2006**, *8*, 1985.

(50) Cheng, B.-M.; Grover, J. R.; Walters, E. A. *Chem. Phys. Lett.* **1995**, *232*, 364.

(51) Feller, D.; Jordan, K. D. *J. Phys. Chem. A* **2000**, *104*, 9971.

JP801693P